Strong anharmonicity and high thermoelectric performance of cubic thallium-based fluoride perovskites $TlXF_3$ (X = Hg, Sn, Pb)

Xuhao Song,[1] Yinchang Zhao,[1,*] Xichang Wang,[1]
Jun Ni,[2,†] Sheng Meng,[3,4,‡] and Zhenhong Dai[1,§]

[1]*Department of Physics, Yantai University,*
Yantai 264005, People's Republic of China
[2]*Department of Physics, Tsinghua University,*
Beijing 100084, People's Republic of China
[3]*Beijing National Laboratory for Condensed Matter Physics and Institute of Physics,*
Chinese Academy of Sciences, Beijing,
100190, People's Republic of China
[4]*Collaborative Innovation Center of Quantum Matter,*
Beijing 100084, People's Republic of China

(Dated: January 12, 2023)

PACS numbers: 65.40.-b, 66.70.-f, 63.20.-e, 72.20.-i

Keywords: first-principles calculation, anharmonic renormalization, lattice thermal conductivity, electrical transport, thermoelectric material

A. S1.

For calculating the phonon and thermal transport properties, the interatomic force constants are captured from the ALAMODE code. First, we captured the second-order IFCs by virtue of the finite-displacement approach in a 2×2×2 supercell with displacement of 0.01 Å. We then used the compressive sensing lattice dynamics approach to obtain cubic and quartic IFCs. More specifically, we first simulated 4000-step ab initio molecular dynamics at room temperature with 2-fs time steps in 2×2×2 supercells to sample 80 snapshots. On this basis, each sample moves all atoms by 0.1 Å random directions to obtain a quasi-random configuration. Next, we use static DFT in a 5×5×5 k-point grid to compute the Hellmann Feynman force for each quasi-random configuration. At last, we use the least absolute shrinkage and selection operator technique to compute anharmonic IFCs from the displacement and force composition dataset extracted from 80 quasi-random configurations.

In the calculation of harmonic IFCs, the interactions between all atoms in the supercell are considered, and the fifth and fourth nearest neighbor interactions are selected for the calculation of third- and fourth-order IFCs. The third and second nearest neighbor interactions are then taken into account because the fifth- and sixth-order IFCs wont significantly alter the results.

Based on the relaxation time approximation, the κ_L tensor is written as

$$\kappa_L = \kappa_L^{\alpha\beta}(\mathrm{T}) = \frac{1}{N\Omega}\sum_{q,j} C_{q,j}(T) v_{q,j}^{\alpha} v_{q,j}^{\beta} \tau_{q,j}(\mathrm{~T}), \tag{S1}$$

in which α and β denote Cartesian coordinates directions; N and Ω are the number of wave vectors and volume of the unit cell, respectively; q and j are the sign of phonon modes; $C_{q,j}$, $v_{q,j}^{\alpha(\beta)}$ and $\tau_{q,j}(\mathrm{T})$ are the specific heat capacity, the phonon group velocity, and the lifetime of the phonons, respectively.

Based on the Matthiessens rule, the total τ_{ph} can be written as is

$$\tau_{\mathrm{ph}}^{-1}(\mathrm{T}) = 2\left(\Gamma_{\mathrm{ph}}^{anh}(\mathrm{~T}) + \Gamma_{\mathrm{ph}}^{iso} + \frac{|v_{\mathrm{ph}}|}{L}\right), \tag{S2}$$

where $\Gamma_{\mathrm{ph}}^{anh}(\mathrm{~T})$ is cubic anharmonic phonon linewidth, $\Gamma_{\mathrm{ph}}^{iso}$ is isotope effect phonon linewidth, and L is grain boundary size, respectively.

The electrical transport coefficients including S, σ, and κ_e are expressed as

$$\sigma_{\alpha\beta} = e^2 \int \Sigma_{\alpha\beta}(\varepsilon)[-\frac{\partial f^0}{\partial \varepsilon}]d\varepsilon, \tag{S3}$$

$$S_{\alpha\beta} = \frac{1}{eT}\frac{\int \Sigma_{\alpha\beta}(\varepsilon)(\varepsilon-\varepsilon_F)[-\frac{\partial f^0}{\partial \varepsilon}]d\varepsilon}{\int \Sigma_{\alpha\beta}(\varepsilon)[-\frac{\partial f^0}{\partial \varepsilon}]d\varepsilon}, \tag{S4}$$

$$\kappa_{\alpha\beta} = \frac{1}{T}\{\frac{(\int \Sigma_{\alpha\beta}(\varepsilon)(\varepsilon-\varepsilon_F)[-\frac{\partial f^0}{\partial \varepsilon}])^2 d\varepsilon}{\int \Sigma_{\alpha\beta}(\varepsilon)[-\frac{\partial f^0}{\partial \varepsilon}]d\varepsilon} - \int \Sigma_{\alpha\beta}(\varepsilon)(\epsilon-\varepsilon_F)^2[\frac{\partial f^0}{\partial \varepsilon}]d\epsilon\}, \tag{S5}$$

in which e, T, ε_F, $\sum_{\alpha\beta}(\varepsilon)$ and f^0 is electron charge, temperature, Fermi level of a certain doping, spectral conductivity and Fermi-Dirac distribution function, respectively.

The spectral conductivity is defined as

$$\Sigma_{\alpha\beta}(\varepsilon) = \sum_n \int \frac{d\mathbf{k}}{8\pi^3} \upsilon_{n\mathbf{k},\alpha}\upsilon_{n\mathbf{k},\beta}\tau_{n\mathbf{k}}\delta(\varepsilon-\varepsilon_{n\mathbf{k}}), \tag{S6}$$

where n is the band index, $\mathbf{k}$ is wave vector, α and β denote Cartesian coordinates, $\varepsilon_{n\mathbf{k}}$ is the energy and $\upsilon_{n\mathbf{k},\alpha}$ is carrier group velocity.

For electronic relaxation lifetime, multiple scattering mechanisms are considered, including acoustic deformation potential scattering, polar optical phonon scattering, ionized impurity scattering, and boundary scattering, which were calculated from materials parameters obtained from first principles. In particular, The differential scattering rate from state $\psi_{n\mathbf{k}}$ to state $\psi_{m\mathbf{k}+\mathbf{q}}$ is calculated using Fermi's golden rule as

$$\tilde{\tau}^{-1}_{n\mathbf{k}\to m\mathbf{k}+\mathbf{q}} = \frac{2\pi}{\hbar}|g_{nm}(\mathbf{k},\mathbf{q})|^2\delta(\varepsilon_{n\mathbf{k}}-\varepsilon_{m\mathbf{k}+\mathbf{q}}), \tag{S7}$$

where $\varepsilon_{n\mathbf{k}}$ is the energy of state $\psi_{n\mathbf{k}}$, and $g_{nm}(\mathbf{k},\mathbf{q})$ is the matrix element for scattering from state $\psi_{n\mathbf{k}}$ into state $\psi_{m\mathbf{k}+\mathbf{q}}$.

The acoustic deformation potential matrix element is given by

$$g^{ADP}(\mathbf{k},\mathbf{q}) = [\frac{k_B T \varepsilon_d^2}{B}]^{\frac{1}{2}} < \psi_{\mathbf{k}+\mathbf{q}}|\psi_{\mathbf{k}} >, \tag{S8}$$

where k_B is the Boltzmann constant, T is the temperature of material, ϵ_d is the volume-deformation potential at the valence band maximum, B is the bulk modulus. The polar optical phonon differential scattering rate is given by

$$g^{POP}(\mathbf{k},\mathbf{q}) = [\frac{\hbar\omega_{po}}{2}(\frac{1}{\epsilon_\infty}-\frac{1}{\epsilon_s})]\frac{< \psi_{\mathbf{k}+\mathbf{q}}|\psi_{\mathbf{k}} >}{|\mathbf{q}|}, \tag{S9}$$

where $\hbar$ is the reduced Planck constant, ω_{po} is an effective optical phonon frequency, ϵ_∞ is the high-frequency dielectric constant, ϵ_s is the static dielectric constant. The ionized impurity scattering rate can be written as

$$g^{IMP}(\mathbf{k},\mathbf{q}) = [\frac{e^2 n_{ii}}{\varepsilon_s^2}]\frac{< \psi_{\mathbf{k}+\mathbf{q}}|\psi_{\mathbf{k}} >}{|\mathbf{q}|^2+\beta^2}, \tag{S10}$$

TABLE S1. The material parameters for $\mathrm{TlXF_3}$ (X = Hg, Sn, Pb) used in AMSET calculations of electronic transport properties. The ϵ_s and ϵ_∞ are the static dielectric constants and high-frequency dielectric constants, respectively. The ω_{po} is the effective polar optical phonon frequency.

semiconductor	ϵ_s	ϵ_∞	ω_{po}(THz)
$\mathrm{TlHgF_3}$	5.16	3.62	4.49
$\mathrm{TlSnF_3}$	11.53	4.81	2.28
$\mathrm{TlPbF_3}$	11.34	3.47	5.41

where e is the electron charge, β is the inverse screening length calculated from the density of states, n_{ii} is the concentration of ionized impurities. The above parameters can be calculated by first principles. Since the exact ionized impurity concentration cannot be determined, the concentration is set equal to the number of free carriers. Additionally, boundary scattering rate is set to v_g/L, where v_g is the electron group velocity and L is the mean free path in nm.

Finally, the rational carrier relaxation time can be calculated, the τ as

$$\frac{1}{\tau^{\mathrm{tot}}} = \frac{1}{\tau^{\mathrm{ADP}}} + \frac{1}{\tau^{\mathrm{IMP}}} + \frac{1}{\tau^{\mathrm{POP}}} + \frac{1}{\tau^{\mathrm{MFP}}}, \tag{S11}$$

where ADP, POP, IMP and MFP are the scattering rates of the completely anisotropic acoustic deformation potential, the scattering rates of the polar optical phonon, the scattering rates of ionized impurity, and boundary scattering rates, respectively.

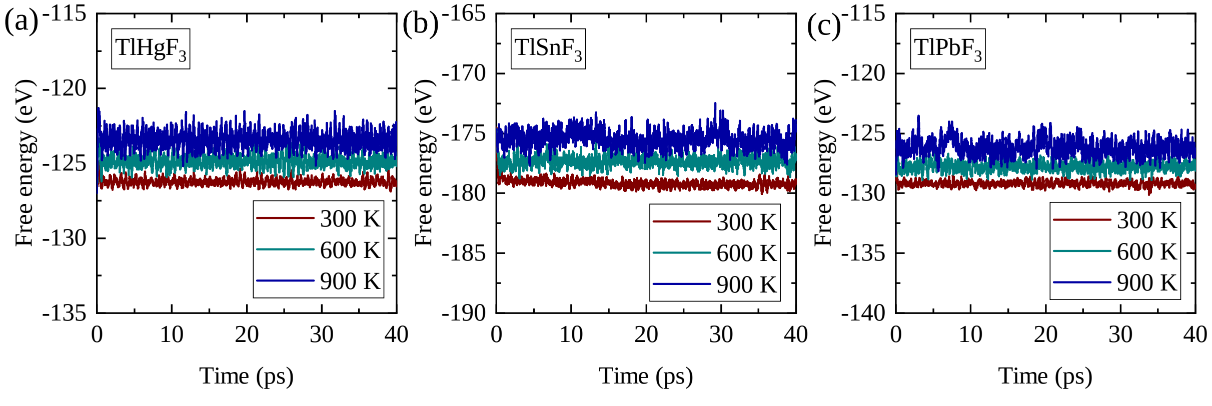

Fig. S1. (Color online). The free energy as the function of time for the cubic (a) $\mathrm{TlHgF_3}$, (b) $\mathrm{TlSnF_3}$ and (c) $\mathrm{TlPbF_3}$ by using the AIMD simulations. Wine red, dark cyan, and royal blue lines represent 300 K, 600 K, and 900 K respectively.

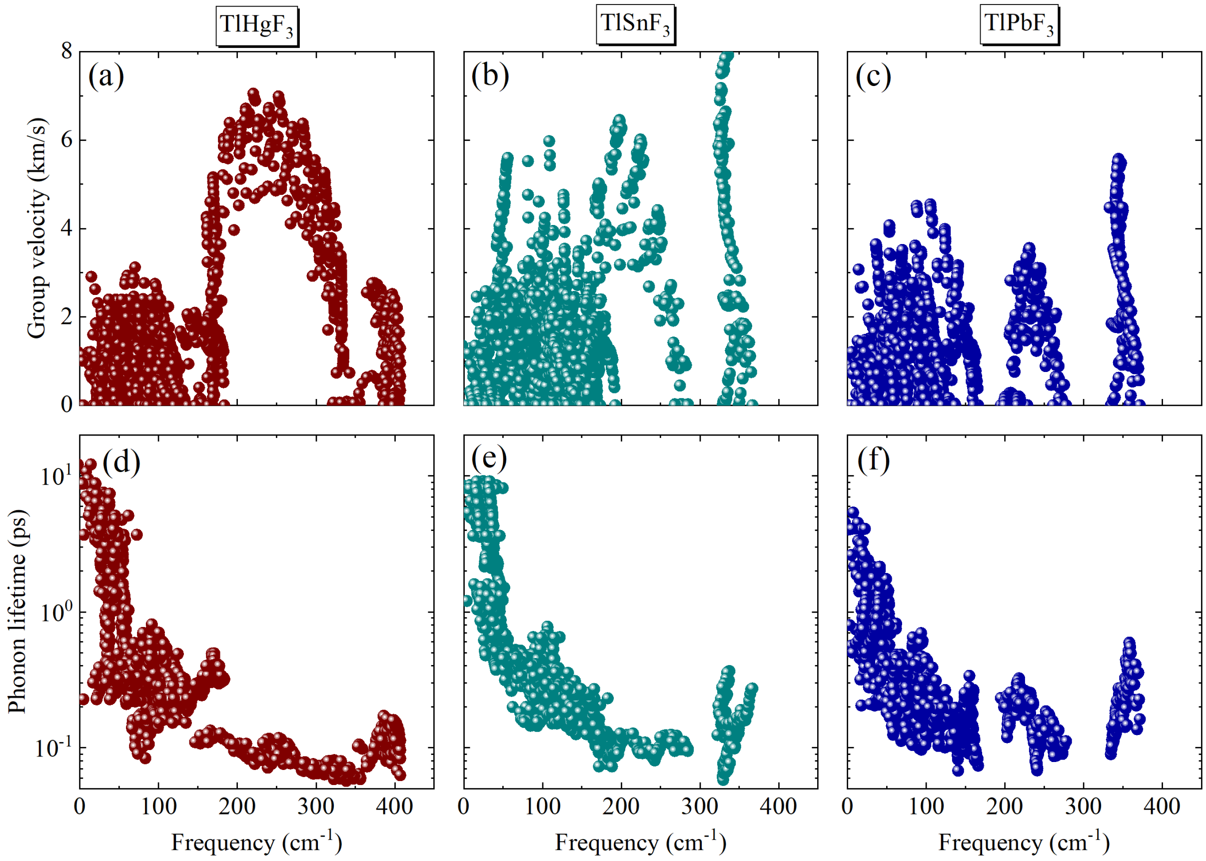

Fig. S2. (Color online). Phonon group velocities of (a) TlHgF$_3$, (b) TlSnF$_3$, and (c) TlPbF$_3$ at 300 K. Phonon lifetimes of (d) TlHgF$_3$, (e) TlSnF$_3$, and (f) TlPbF$_3$ at 300 K. Wine red, dark cyan, and royal blue solid balls represent TlHgF$_3$, TlSnF$_3$, and TlPbF$_3$, respectively.

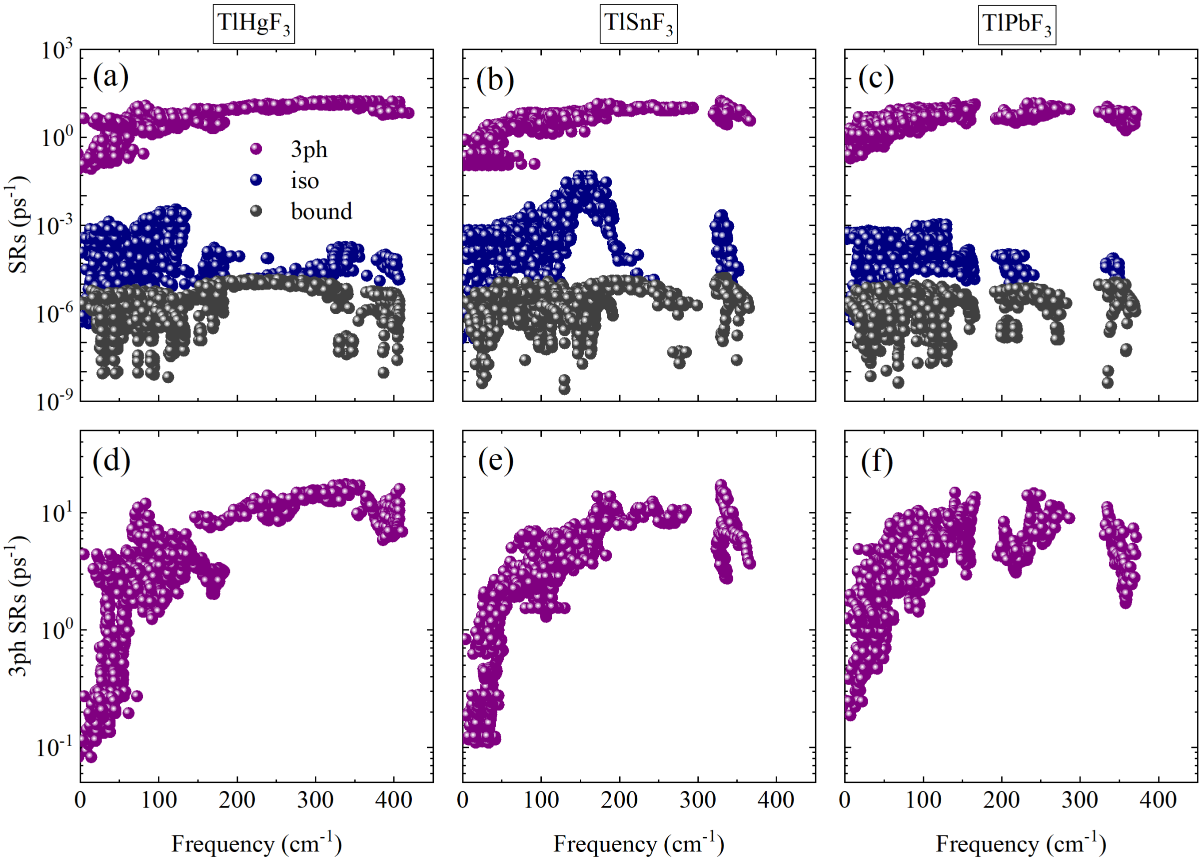

Fig. S3. (Color online). Scattering rates of (a) TlHgF$_3$, (b) TlSnF$_3$, and (c) TlPbF$_3$ at 300 K, where purple, navy, and dark gray represent three-phonon (3ph) scattering, isotope (iso) scattering, and grain boundary (bound) scattering, respectively. Three-phonon scattering rates at 300 K for (d) TlHgF$_3$, (e) TlSnF$_3$, and (f) TlPbF$_3$.

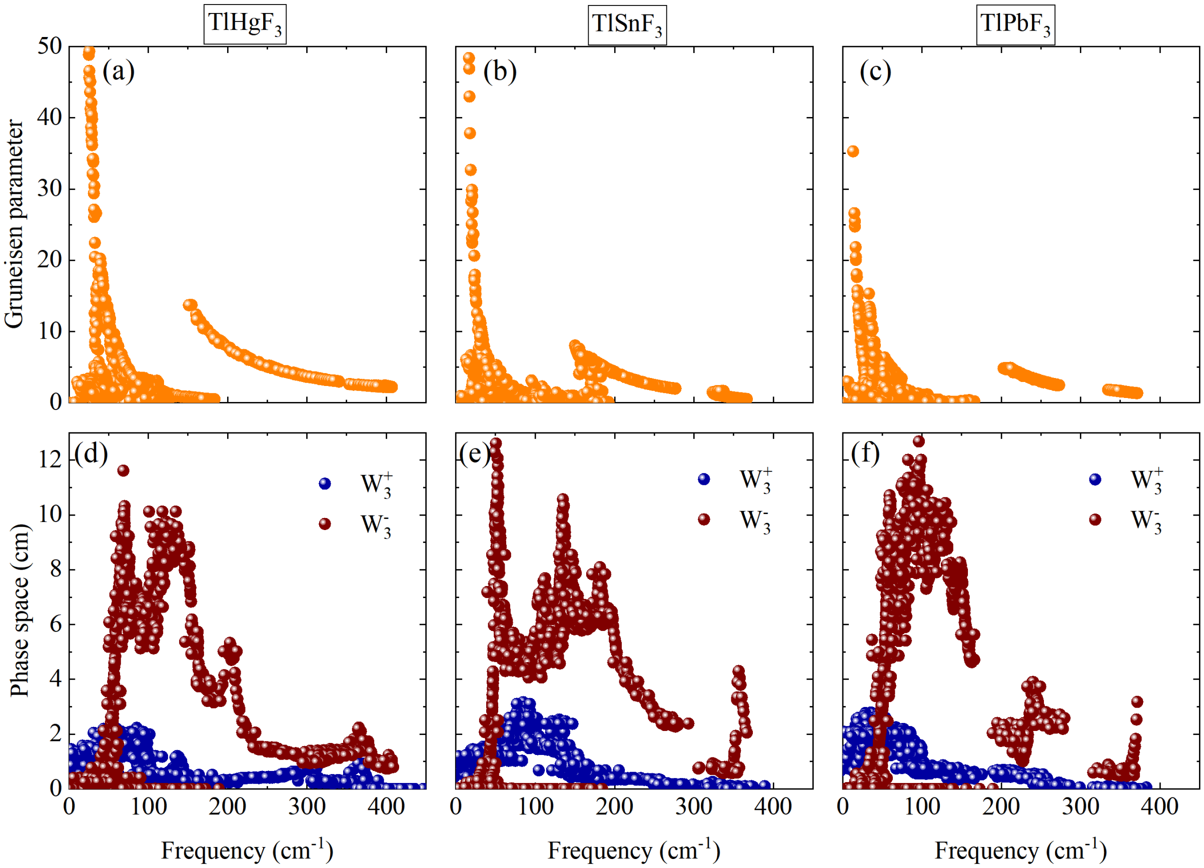

Fig. S4. (Color online). Grüneisen parameter of (a) TlHgF$_3$, (b) TlSnF$_3$, and (c) TlPbF$_3$ at 300 K. Three-phonon scattering phase space at 300 K for (d) TlHgF$_3$, (e) TlSnF$_3$, and (f) TlPbF$_3$, where royal blue and wine red indicate excitation (W_3^+) and absorption (W_3^-) processes, respectively.

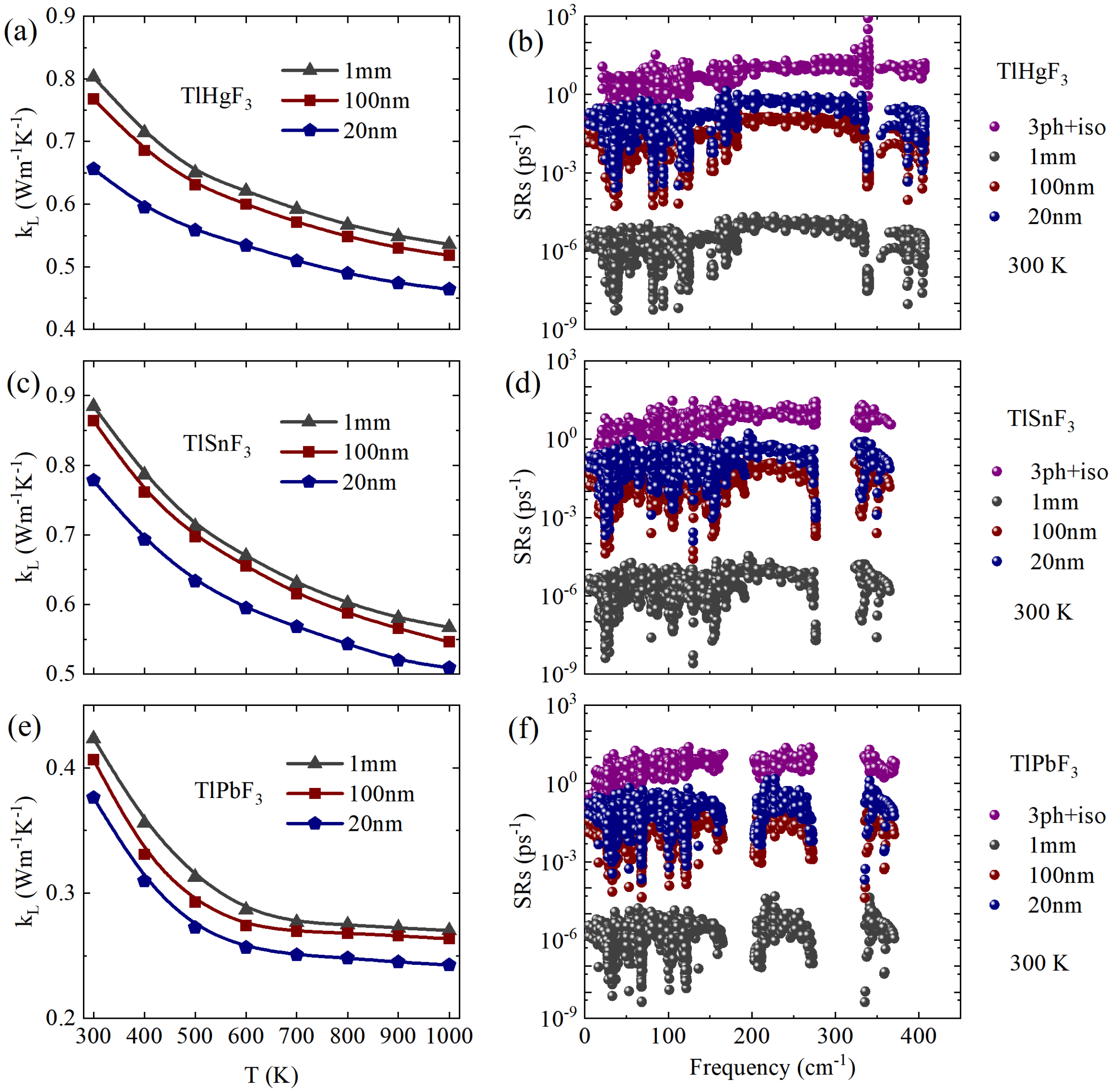

Fig. S5. (Color online). The lattice thermal conductivities of (a) TlHgF$_3$, (c) TlSnF$_3$, and (e) TlPbF$_3$ at different grain boundary sizes, where dark grey, wine red, and royal blue represent sizes of 1 mm, 100 nm, and 20 nm, respectively. Comparison of boundary scattering rates and other scattering rates for (b) TlHgF$_3$, (d) TlSnF$_3$, and (f) TlPbF$_3$ at different grain boundary sizes. Dark gray, burgundy, and royal blue solid spheres represent dimensions of 1 mm, 100 nm, and 20 nm, respectively. The purple solid sphere represents the sum of the three-phonon scattering rate and the isotope scattering rate.

TABLE S2. The calculated isotropic poisson's ratio ν, Pughs ratio B/G, universal elastic anisotropy A^U, and band gaps E_g for perovskites $TlXF_3$ (X = Hg, Sn, Pb).

semiconductor	ν	B/G	A^U	E_g^{PBE}	E_g^{HSE06}
$TlHgF_3$	0.39	4.22	2.06	1.47	3.02
$TlSnF_3$	0.35	2.94	2.24	0.58	1.14
$TlPbF_3$	0.35	2.91	3.75	1.78	2.58

TABLE S3. Charge transfer is calculated using Bader charge analysis. ΔQ stands for charge transfer; a positive value means gaining charge, and a negative value means losing charge.

semiconductor	ΔQ (Tl)	ΔQ (X)	ΔQ (F)
$TlHgF_3$	-0.89	-1.32	0.74
$TlSnF_3$	-0.84	-1.61	0.81
$TlPbF_3$	-0.86	-1.59	0.82

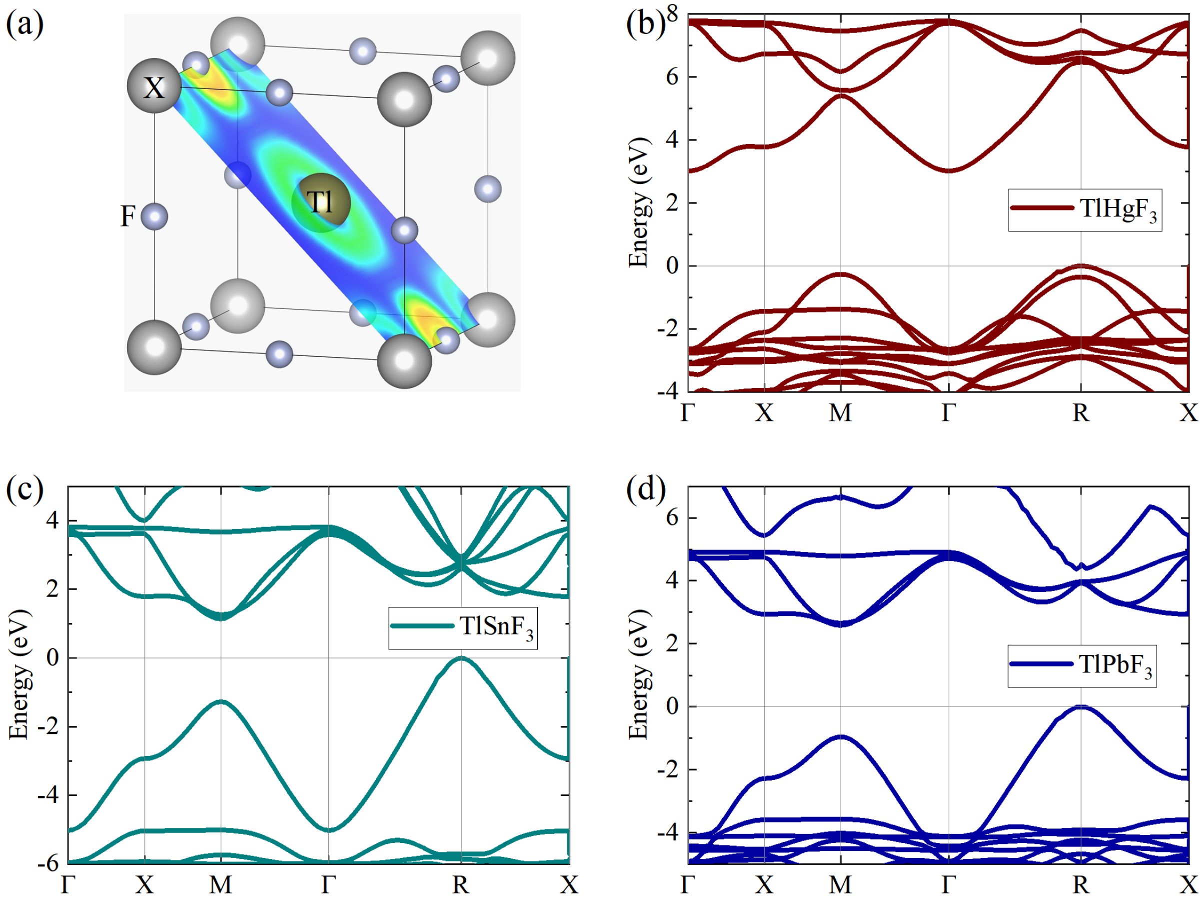

Fig. S6. (Color online). (a) The (011) surface is displayed in an intuitive position in a three-dimensional stereogram. The electronic band structures by using the HSE06 exchange-correction functional for (b) $TlHgF_3$, (c) $TlSnF_3$ and (d) $TlPbF_3$.

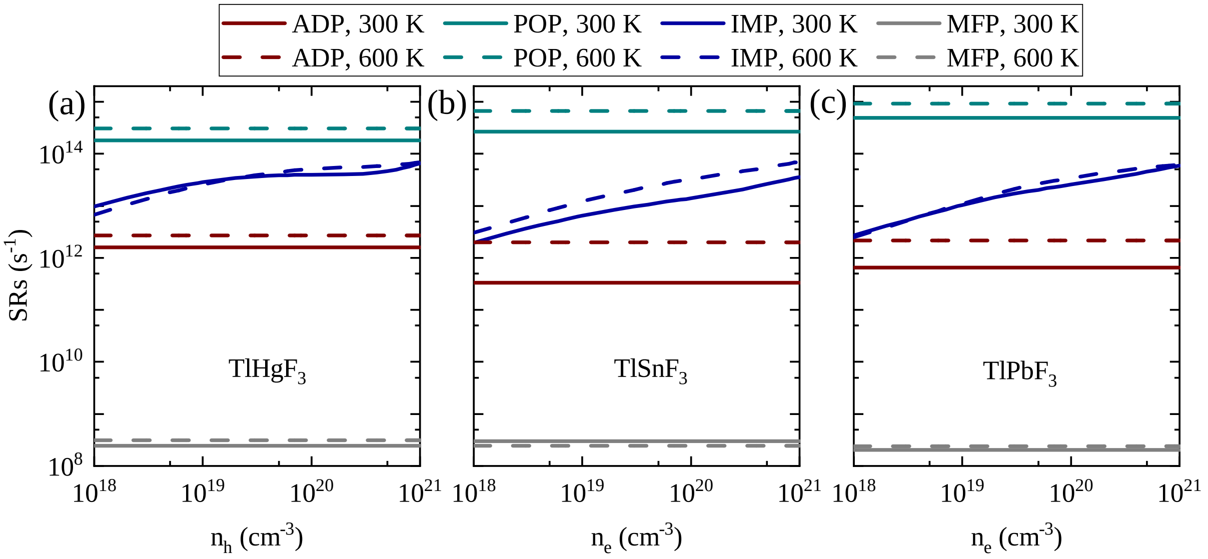

Fig. S7. (Color online). The electron scattering rate of p-type (a) $TlHgF_3$, n-type (b) $TlSnF_3$ and (c) $TlPbF_3$. ADP, POP, IMP, and MFP represent the acoustic deformation potential scattering, polar-optical phonon scattering, ionized impurity scattering, and electron grain boundary scattering. The solid lines represent the 300 K, and dash lines represent the 600 K.

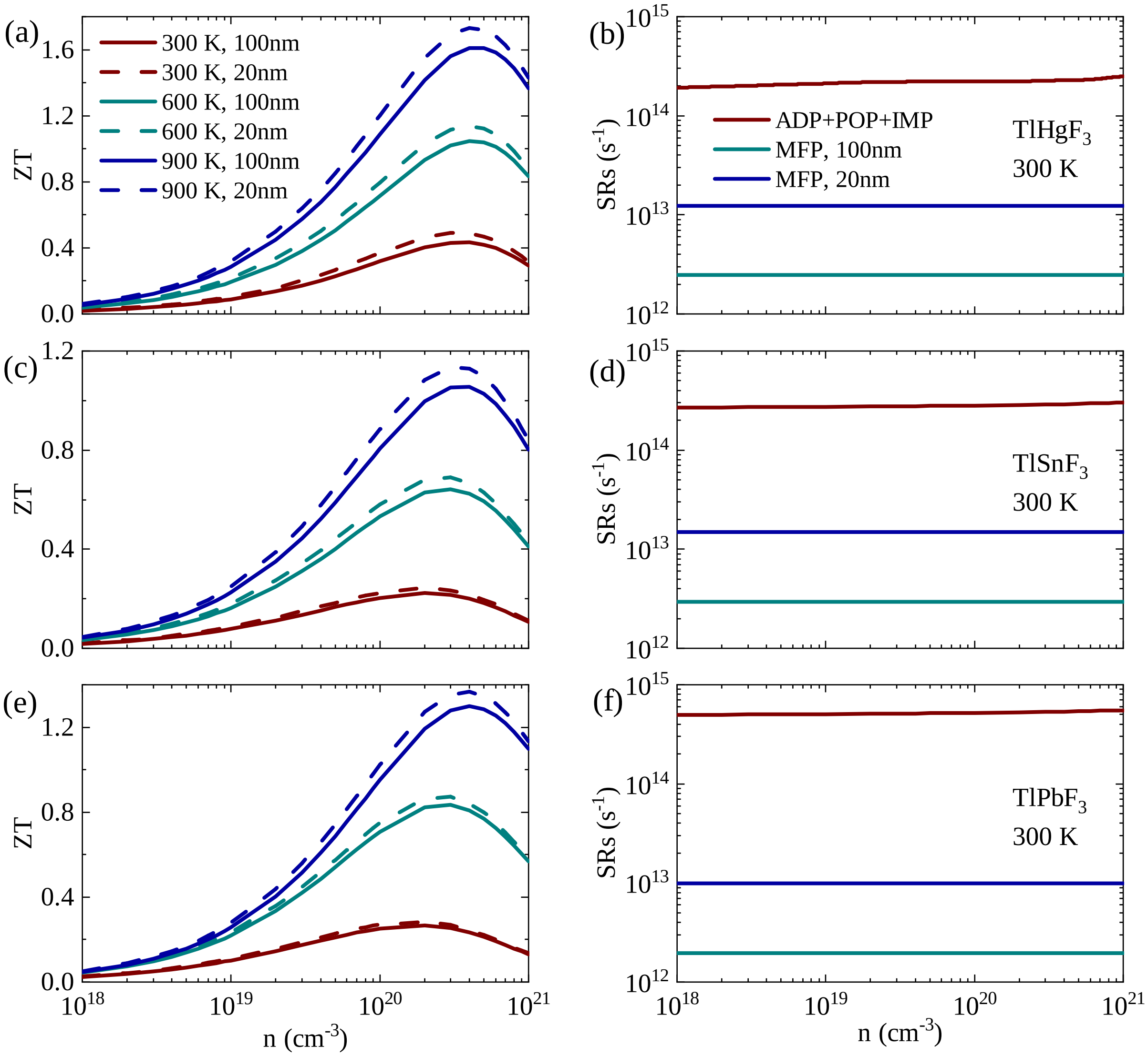

Fig. S8. (Color online). Thermoelectric figure of merit (ZT) and electronic grain boundary scattering rates (SRs) at different grain boundary sizes. For the ZT values of (a) $TlHgF_3$, (c) $TlSnF_3$, and (e) $TlPbF_3$, wine red, dark cyan, and royal blue are indicated at 300 K, 600 K, and 900 K, respectively. The solid and dashed lines represent grain boundary sizes of 100 nm and 20 nm, respectively. For the SRs of (b) $TlHgF_3$, (d) $TlSnF_3$, and (f) $TlPbF_3$, wine red, dark cyan, and royal blue represent the sum of the other three scattering rates, electron grain boundary scattering at 100 nm and 20 nm, respectively.

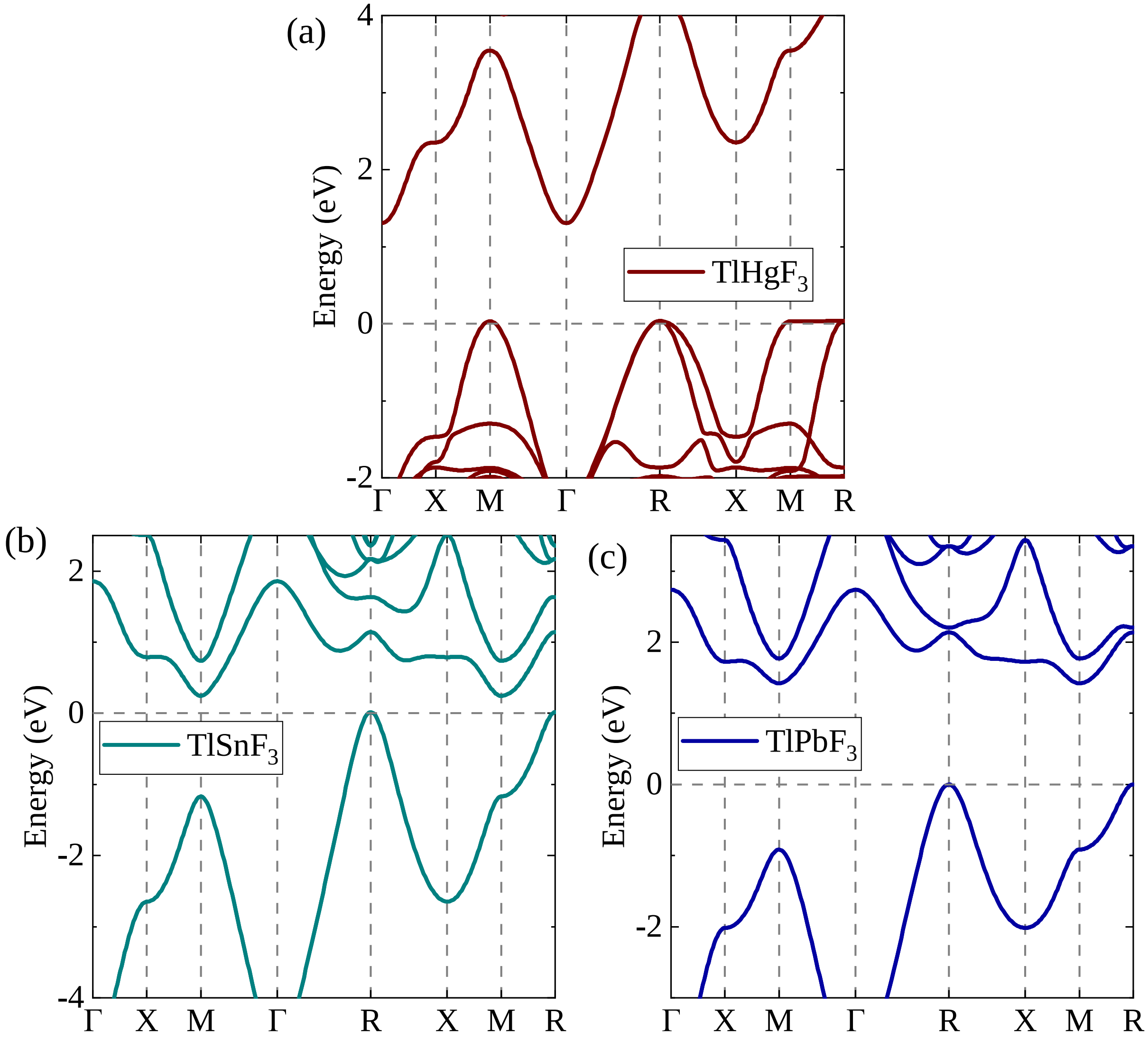

Fig. S9. (Color online). The electronic band structures of (a) $TlHgF_3$, (b) $TlSnF_3$ and (c) $TlPbF_3$ calculated by PBE functional after considering spin-orbit coupling.

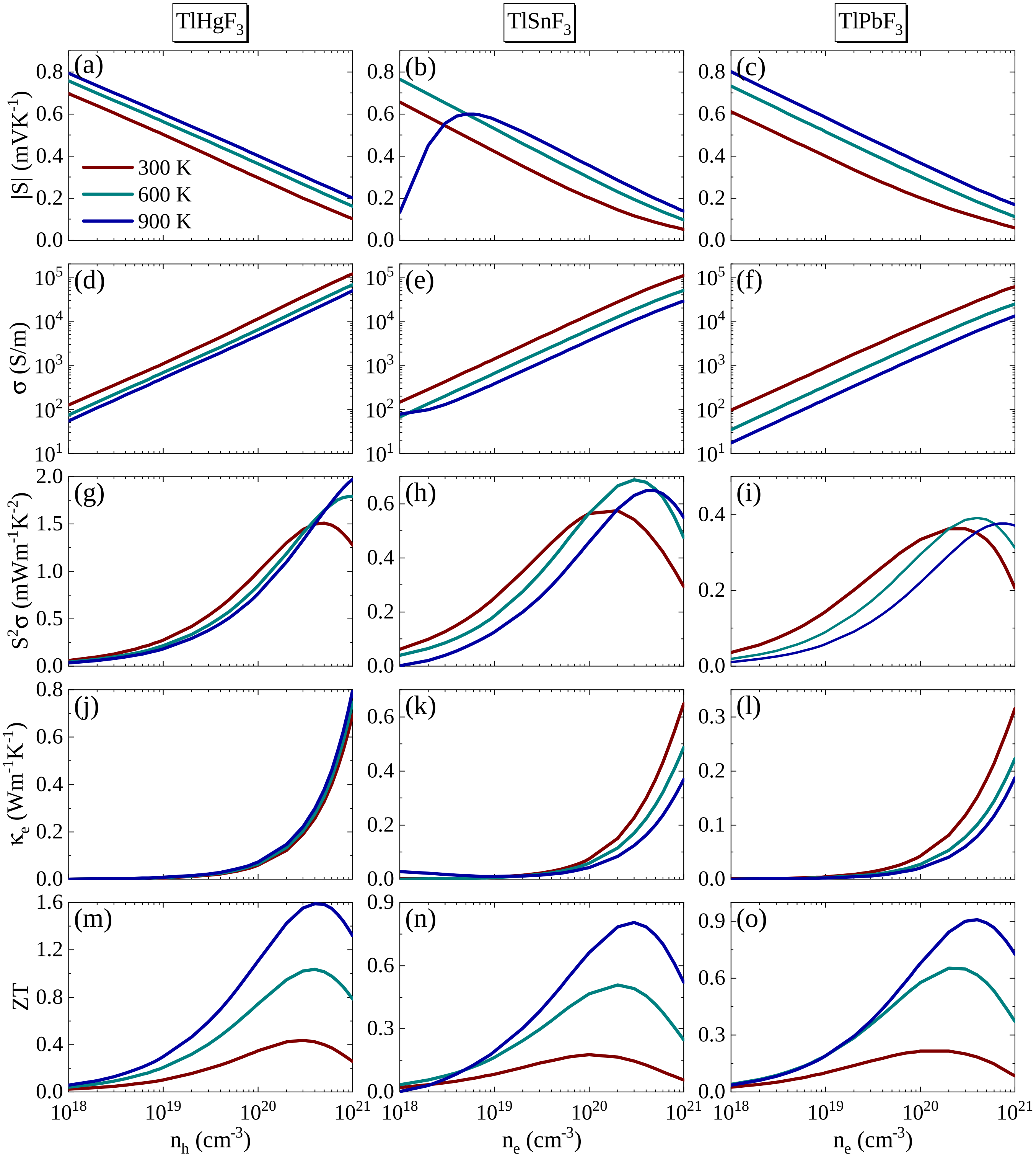

Fig. S10. (Color online). The electron transport coefficients of p-type $\mathrm{TlHgF_3}$ (left), n-type $\mathrm{TlSnF_3}$ (middle), and $\mathrm{TlPbF_3}$ (right) after considering spin-orbit coupling, including the absolute value of the Seebeck coefficient $|S|$ (a, b, and c), electrical conductivity σ (d, e, and f), power factor $S^2\sigma$ (g, h, and i), electronic thermal conductivity κ_e (j, k, and l), and the thermoelectric figure of merit ZT (m, n, and o). The wine red, dark cyan, and royal blue lines are indicated at 300 K, 600 K, and 900 K, respectively.

---

[*] y.zhao@ytu.edu.cn

[†] junni@tsinbghua.edu.cn

[‡] smeng@iphy.ac.cn

[§] zhdai@ytu.edu.cn